

## Localization and Characterization of the Inhibitory $\text{Ca}^{2+}$ -binding Site of *Physarum polycephalum* Myosin II\*

Received for publication, April 22, 2003

Published, JBC Papers in Press, May 16, 2003, DOI 10.1074/jbc.M304220200

László Farkas‡, András Málnási-Csizmadia‡, Akio Nakamura§, Kazuhiro Kohama§, and László Nyitrai‡¶

From the ‡Department of Biochemistry, Eötvös Loránd University, Budapest 1117, Hungary and §Department of Pharmacology, Gunma University School of Medicine, Maebashi, Gunma 371, Japan

A myosin II is thought to be the driving force of the fast cytoplasmic streaming in the plasmodium of *Physarum polycephalum*. This regulated myosin, unique among conventional myosins, is inhibited by direct  $\text{Ca}^{2+}$  binding. Here we report that  $\text{Ca}^{2+}$  binds to the first EF-hand of the essential light chain (ELC) subunit of *Physarum* myosin. Flow dialysis experiments of wild-type and mutant light chains and the regulatory domain revealed a single binding site that shows moderate specificity for  $\text{Ca}^{2+}$ . The regulatory light chain, in contrast to regulatory light chains of higher eukaryotes, is unable to bind divalent cations. Although the  $\text{Ca}^{2+}$ -binding loop of ELC has a canonical sequence, replacement of glutamic acid to alanine in the  $-\alpha$  coordinating position only slightly decreased the  $\text{Ca}^{2+}$  affinity of the site, suggesting that the  $\text{Ca}^{2+}$  coordination is different from classical EF-hands; namely, the specific “closed-to-open” conformational transition does not occur in the ELC in response to  $\text{Ca}^{2+}$ .  $\text{Ca}^{2+}$ - and  $\text{Mg}^{2+}$ -dependent conformational changes in the microenvironment of the binding site were detected by fluorescence experiments. Transient kinetic experiments showed that the displacement of  $\text{Mg}^{2+}$  by  $\text{Ca}^{2+}$  is faster than the change in direction of cytoplasmic streaming; therefore, we conclude that  $\text{Ca}^{2+}$  inhibition could operate in physiological conditions. By comparing the *Physarum*  $\text{Ca}^{2+}$  site with the well studied  $\text{Ca}^{2+}$  switch of scallop myosin, we surmise that despite the opposite effect of  $\text{Ca}^{2+}$  binding on the motor activity, the two conventional myosins could have a common structural basis for  $\text{Ca}^{2+}$  regulation.

Myosins constitute a diverse superfamily of motor proteins providing the driving force in muscle contraction and many forms of actin-based cellular motility. They are typically constructed of three functional domains, which are the motor domain, the neck or light chain binding domain, and a unique tail region that in many myosins forms a coiled-coil dimer. The heavy chain segment in the neck region consists of repeats of  $\alpha$ -helical sequences called IQ motifs, each of which binds and is stabilized by one light chain subunit. In conventional myosins (myosin II class) the regulatory light chain (RLC)<sup>1</sup> and ELC

bind to two tandem IQs, whereas in non-conventional myosins CaM and/or CaM-like proteins bind to one to six tandem IQ motifs (1). Because the neck region is involved in the regulation of many myosins, it is often referred to as the regulatory domain (RD). The light chains belong to the EF-hand family of  $\text{Ca}^{2+}$ -binding proteins, including CaM, the ubiquitous eukaryotic  $\text{Ca}^{2+}$  sensor. CaM has four  $\text{Ca}^{2+}$ -binding sites, a pair of EF-hands in both the N- and C-terminal domains (lobes); however, most of the divalent cation-binding sites of ELC and RLC have been lost during evolution (2).

Enzymatic and motor activity in the myosin superfamily can be controlled by a variety of mechanisms and regulatory systems associated with either the actin filament or the myosin molecule. Regulation through the RD can be achieved by reversible phosphorylation or direct  $\text{Ca}^{2+}$  binding. Vertebrate smooth muscle and non-muscle myosin IIs are activated by phosphorylation of the RLC by a  $\text{Ca}^{2+}$ /CaM-dependent myosin light chain kinase (3). In the animal kingdom the Mollusca conventional myosins are unique in that they are activated by direct  $\text{Ca}^{2+}$  binding to the ELC (4). In the lower eukaryote *Physarum polycephalum*, in contrast to any other known conventional myosins, increase in  $\text{Ca}^{2+}$  concentration inhibits the activity of myosin (5, 6). The diverse classes of unconventional myosins are also regulated in part by the interaction of  $\text{Ca}^{2+}$  with the CaM subunits; the consequences of the  $\text{Ca}^{2+}$  binding can be more complex and are not as well understood as in the myosin II class. Elevated  $\text{Ca}^{2+}$  concentration has, in general, an inhibitory effect on the motility of vertebrate myosin I and myosin V as well as the plant-specific myosins (7–9).

Structural studies of the isolated RD (a three-chain complex of ELC, RLC, and a  $\sim 10$ -kDa fragment of the heavy chain) of scallop myosin II revealed that the triggering  $\text{Ca}^{2+}$ -binding site is localized in the first EF-hand of ELC (10, 11). The conformation of the N-terminal domain of ELC containing the bound  $\text{Ca}^{2+}$  is closed rather than open, which is found in the conventional  $\text{Ca}^{2+}$ -saturated EF-hands. RLC of scallop and all the known higher eukaryotic myosin II contains a divalent metal-binding site in the first EF-hand that preferentially binds  $\text{Mg}^{2+}$  and has only a structural role (10, 11).

Cytoplasmic streaming in plasmodia of the myxomycete *P. polycephalum* is exceedingly vigorous. The cytoplasm streams at a rate about 1.3 mm/s and changes direction every 2–3 min. This oscillatory process is regulated by  $\text{Ca}^{2+}$  and is

\* This work was supported by National Scientific Research Fund Grant OTKA T32443 and the Japan Society for the Promotion of Science. The costs of publication of this article were defrayed in part by the payment of page charges. This article must therefore be hereby marked “advertisement” in accordance with 18 U.S.C. Section 1734 solely to indicate this fact.

¶ To whom correspondence should be addressed: Dept. of Biochemistry, Eötvös Loránd University, Budapest, Pázmány P. sétány 1/C, H-1117. Tel.: 361-381-2171; Fax: 361-381-2172; E-mail: nyitrai@cerberus.elte.hu.

<sup>1</sup> The abbreviations used are: RLC, regulatory light chain; ELC, essential light chain; CaM, calmodulin; RD, regulatory domain; HC,

heavy chain; E26A ELC, *Physarum* ELC containing point mutation E26A; D15A/D17A/E26A ELC, *Physarum* ELC containing point mutations D15A, D17A, and E26A; E97A ELC, *Physarum* ELC containing point mutation E97A; S124A/D126A ELC, *Physarum* ELC containing point mutations S124A/D126A; 1,5-IAEDANS, 5-(((2-iodoacetyl)amino)ethyl)amino naphthalene-1-sulfonic acid;  $k_{\text{off}}$ , dissociation rates constant;  $k_{\text{on}}$ , second order rate constant for divalent cation binding; MOPS, 3-morpholinopropanesulfonic acid; DTT, dithiothreitol.

thought to be driven by a conventional myosin (12).  $\text{Ca}^{2+}$  regulates the contractile system of *Physarum* plasmodia by direct binding to the myosin, and inhibiting its ATPase activity and *in vitro* motility (5, 6). It was proposed that the ELC is the  $\text{Ca}^{2+}$ -binding subunit of *Physarum* myosin (13–15). Other mechanisms could also be involved in the regulation or modulation of the activity of the myosin. Phosphorylation of the heavy chain and RLC by heavy chain and light chain kinases, respectively, increases the affinity of myosin to actin; activity of the kinases is suppressed by  $\text{Ca}^{2+}$ ; however, at high actin concentrations existing *in vivo* in the plasmodium, phosphorylation has a negligible effect on regulation of myosin (6). A caldesmon-like actin-binding protein can stimulate the ATPase activity of myosin. This effect is inhibited by  $\text{Ca}^{2+}$ -CaM (16, 17).

To compare the structural basis of the two, oppositely regulated  $\text{Ca}^{2+}$ -binding conventional myosins, we initiated studies to localize and characterize the regulatory calcium-binding site of *Physarum* myosin using recombinant LCs and RD. The results reveal that there is one  $\text{Ca}^{2+}$ -binding site per head in the myosin. By mutating all of the EF-hands, which were predicted to be competent metal-binding sites based on sequence analysis, we demonstrate that the first EF-hand of the ELC is responsible for  $\text{Ca}^{2+}$  binding. Moreover, our results suggest that the N-terminal domain of ELC remains in a closed conformation even in the presence of  $\text{Ca}^{2+}$ .

#### EXPERIMENTAL PROCEDURES

**Wild-type and Mutant Expression Constructs**—Total RNA from *P. polycephalum* plasmodia (strain Ng-1) was obtained by the acid-guanidium-phenol-chloroform method (18). Purification of RNA and cDNA synthesis was performed as reported earlier (19). cDNAs encoding the RLC and the heavy chain were cloned by PCR using degenerate oligonucleotides designed on the basis of partial peptide sequencing of the isolated myosin subunits and conserved regions within the myosin motor domain (GenBank™ accession numbers AB076705 and AF335500). Details of the cloning procedure will be published elsewhere. *Dictyostelium* ELC was cloned by PCR based on published sequence (GenBank™ accession number X54161) using total RNA isolated from AX2 cell line. The cDNAs of RLC, ELC, the N- and C-terminal domains of ELC (residues 1–77 and 73–147), the HC fragment of the RD (residues 771–841), and *Dictyostelium* ELC were subcloned into the expression vectors pET15b or pET21a (Novagen) between the *NdeI* and *BamHI* sites. Restriction sites for cloning of the cDNA fragments were introduced by PCR. The pET15b constructs contain an N-terminal fusion His<sub>6</sub>-tag sequence. To produce RD, an expression vector was constructed containing sequences of all the three chains with three separate promoters. The pET15b/HC construct was digested with restriction enzymes *BglII* and *BamHI*, and the resulting 370-bp fragment containing the sequence of the T7 promoter and the HC fragment of RD was inserted into the unique *BamHI* site of pET21a/ELC construct. In a similar way, a third sequence cassette containing the RLC-coding sequence together with the T7 promoter was subcloned from pET21a/RLC into the *BamHI* sites of pET21a/ELC vector. In the three-insert construct, only the HC fragment is fused to a His<sub>6</sub>-tag sequence. Site-directed mutagenesis of ELC was performed by PCR using the megaprimer method with the following oligonucleotides: E26A, GTCCATAGAGGCCCTTGGGCAGTGCCC; D15A and D17A, TC-CAGATCTTCGCCAAGGCCCAATGACGGCAAG; E97A, CAAGAGCT-GTCTCAACGCAGCCTCCTGGATG; S124A and D126A, GTTAAT-AGCTCCGGCACCAGCCACAGACACTTCC. All constructs were verified by DNA sequencing.

**Expression and Purification of Recombinant Proteins**—Recombinant proteins were expressed in *Escherichia coli* strain BL21(DE3)pLysS as described previously (19). The light chains were purified under denaturing conditions. Cells were suspended in 6 M guanidine hydrochloride, 0.5 M NaCl, 20 mM sodium phosphate, pH 7.8, 0.5 mM phenylmethylsulfonyl fluoride, 20 μg/ml pepstatin A and homogenized with sonication. The homogenate was centrifuged at 50,000 × g, and the supernatant was loaded onto a Ni<sup>2+</sup> chelate column (ProBond, Invitrogen); the column was washed with a buffer containing 8 M urea, 0.5 M NaCl, 20 mM sodium phosphate at pH 6.0 and 5.3, and the recombinant protein was eluted at pH 4.0. The RD was purified under non-denaturing conditions; cells were suspended in 0.5 M NaCl, 20 mM sodium phosphate, pH 7.8, 3 mM NaN<sub>3</sub>, 0.5 mM phenylmethylsulfonyl fluoride

on ice. After sonication and centrifugation of the homogenate, the supernatant was loaded on a ProBond column and washed with the same buffer at pH 6.0 containing 50 mM imidazole, and the RD was eluted by increasing the concentration of imidazole to 0.5 M. The eluted light chains and RD were dialyzed against 20 mM NaCl, 10 mM Tris/HCl, pH 7.6, 3 mM NaN<sub>3</sub>, 0.1 mM EDTA, 0.1 mM DTT and loaded onto a Mono Q ion exchange column equilibrated with the same buffer. The absorbed proteins were eluted by a linear gradient of NaCl to 0.5 M.

**Purification of *Physarum Myosin***—Plasmodia of *Physarum* were grown on Quaker oatmeal according to Camp (20) with some modifications (21). Myosin was isolated from the collected plasmodia by the high salt extraction method as described earlier (5).

**Calcium Binding Experiments**—The extent of  $\text{Ca}^{2+}$  binding was measured by the flow dialysis method according to Nakashima *et al.* (22, 23) with <sup>45</sup>CaCl<sub>2</sub> (PerkinElmer Life Sciences) in 0.1 M NaCl, 20 mM MOPS/NaOH, pH 7.0, at 25 °C in the presence or absence 2 mM MgCl<sub>2</sub>. The protein concentrations were 25–100 μM. The loss of radioactive ligand during the experiments and the nonspecific  $\text{Ca}^{2+}$  binding to the flow dialysis cell were corrected. In some experiments we measured  $\text{Ca}^{2+}$  binding by equilibrium dialysis as described previously (24) at 22 °C in a buffer containing 50 mM NaCl, 20 mM MOPS/NaOH, pH 7.0, 3 mM NaN<sub>3</sub>, 0.11 mM <sup>45</sup>CaCl<sub>2</sub>, and various concentrations of EGTA to obtain the desired free  $\text{Ca}^{2+}$  concentration. The resulting  $\text{Ca}^{2+}$ -binding data were analyzed by fitting to the Adair-Klotz equation (25) for single binding site,

$$y = \frac{[\text{Ca}^{2+}]}{K_{\text{Ca}^{2+}}} \left( 1 + \frac{[\text{Ca}^{2+}]}{K_{\text{Ca}^{2+}}} \right) + j[\text{Ca}^{2+}] \quad (\text{Eq. 1})$$

where  $K_{\text{Ca}^{2+}}$  is the apparent macroscopic dissociation constant for  $\text{Ca}^{2+}$ ,  $y$  is the number of bound  $\text{Ca}^{2+}$  ions, and  $j$  is the correction factor for nonspecific binding. The macroscopic dissociation constant for  $\text{Mg}^{2+}$  was calculated from  $\text{Ca}^{2+}$ -binding data in the presence of  $\text{Mg}^{2+}$  fitted to the equation describing the competition of  $\text{Ca}^{2+}$  and  $\text{Mg}^{2+}$  for single binding site,

$$y' = \frac{[\text{Ca}^{2+}]K_{\text{Mg}^{2+}}}{K_{\text{Mg}^{2+}}K_{\text{Ca}^{2+}} + K_{\text{Ca}^{2+}}[\text{Mg}^{2+}] + K_{\text{Mg}^{2+}}[\text{Ca}^{2+}] + j[\text{Ca}^{2+}]} \quad (\text{Eq. 2})$$

where  $K_{\text{Mg}^{2+}}$  is the macroscopic dissociation constant for  $\text{Mg}^{2+}$ ,  $K_{\text{Ca}^{2+}}$  is the macroscopic dissociation constant for  $\text{Ca}^{2+}$ ,  $y'$  is the number of bound  $\text{Ca}^{2+}$  ions (mol/mol) at a given  $\text{Mg}^{2+}$  concentration, and  $j$  is the correction factor for nonspecific binding.

**ELC Labeling with 1,5-IAEDANS**—Wild-type and mutant ELCs containing a single cysteine (Cys-10) were labeled with 3-fold molar excess of 1,5-IAEDANS (Sigma-Aldrich) in 6 M guanidine hydrochloride, 10 mM Tris/HCl, pH 7.5, for 30 min at room temperature. Labeling was terminated with 1 mM DTT, and then the samples were dialyzed overnight against a buffer containing 50 mM NaCl, 50 mM HEPES, pH 7.5, 0.1 mM DTT.

**Transient Kinetic Assays**—Transient kinetic assays were performed using an Applied Photophysics SX18MV stopped flow apparatus with a 150 watt Xe lamp at 22 °C. The dead time of the system was 1.5 ms, as determined earlier (26). The assay buffer contained 50 mM NaCl, 50 mM HEPES, pH 7.5, and 0.1 mM DTT. The IAEDANS-labeled ELCs were excited at 336 nm, and the emission was monitored through a GG455 filter.  $\text{Ca}^{2+}$ - and  $\text{Mg}^{2+}$ -saturated IAEDANS-labeled ELCs were rapidly mixed with excess EDTA, respectively.  $\text{Ca}^{2+}$  dissociation from RD were investigated by mixing the  $\text{Ca}^{2+}$ -saturated RD with excess of the calcium indicator Quin 2 (Sigma-Aldrich), which rapidly binds  $\text{Ca}^{2+}$ , reducing the free calcium concentration to nanomolar range. The samples were excited at a wavelength of 366 nm, and the fluorescence was measured through the GG455 filter. During the determination of  $\text{Mg}^{2+}$  dissociation rate from RD by displacement of  $\text{Mg}^{2+}$  with  $\text{Ca}^{2+}$ , the decrease in  $\text{Ca}^{2+}$  concentration was detected by using the low affinity calcium indicator Calcium Green 5N (Molecular Probes). The excitation wavelength was 506 nm, and fluorescence was detected through a 530-nm cut-off filter. All data were collected on a logarithmic time base and analyzed by fitting to exponential functions using Origin, version 5.0 (Microcal Software). Second order rate constants ( $k_{\text{on}}$ ) for  $\text{Ca}^{2+}$  and  $\text{Mg}^{2+}$  binding to ELC and RD were also calculated using the equation,

$$k_{\text{on}} = k_{\text{off}}/K_d \quad (\text{Eq. 3})$$

where  $k_{\text{off}}$  is the dissociation rate constant, determined by transient kinetic measurements, and  $K_d$  is the appropriate macroscopic dissociation constants determined by flow dialysis experiments.

**Steady-state Fluorescence Studies**—Steady-state fluorescence of labeled ELCs was measured at 22 °C in an assay buffer containing 50 mM



TABLE I

Amino acid sequences of the EF-hand loops of *Physarum* ELC, RLC, EF-hand I of *Dictyostelium* ELC and mammalian calmodulin

The amino acids substituted for alanine in the mutant ELCs are boldfaced and italicized. Consensus sequence of the canonical Ca<sup>2+</sup>-binding loop together with the six coordinating residues (x, y, z, -y, -x, -z) is shown below. O, oxygen-containing side group; #, hydrophobic residue; X, any amino acid residue.

<i>Physarum</i> ELC											
EF-1 (15-26)	<b>D</b>	K	<b>D</b>	N	D	G	K	V	S	I	<b>E</b>
EF-2 (41-52)	A	E	L	N	A	K	E	F	D	L	A
EF-3 (86-97)	D	K	E	G	N	G	T	I	Q	E	<b>E</b>
EF-4 (111-122)	S	V	<b>S</b>	G	<b>D</b>	G	A	I	N	Y	E
<i>Dictyostelium</i> ELC											
EF-1 (16-27)	D	K	D	N	D	G	K	V	S	V	E
Mammalian CaM											
EF-1 (19-30)	D	K	D	G	D	G	T	I	T	T	K
<i>Physarum</i> RLC											
EF-1 (29-40)	D	S	E	R	T	G	F	I	T	K	E
Consensus	D	X	O	X	O	G	X	#	O	X	X
	<b>x</b>	<b>y</b>	<b>z</b>	<b>-y</b>	<b>-x</b>	<b>-z</b>					

NaCl, 20 mM MOPS/NaOH, pH 7.2, 0.1 mM DTT using a Spex Fluoromax spectrofluorometer. The samples were excited at 336 nm, and the fluorescence spectra were collected between 450 and 520 nm. Intrinsic Trp fluorescence of *Physarum* RD was measured in the same assay buffer, samples were excited at 297 nm, and fluorescence spectra were collected between 310 and 370 nm. The desired free Ca<sup>2+</sup> (Mg<sup>2+</sup>) concentrations were adjusted by adding 0.1 mM EGTA (EDTA) and the appropriate amount of CaCl<sub>2</sub> (MgCl<sub>2</sub>), calculated by the program ALEX (a gift of Dr. M. Vivaudou).

**Limited Proteolysis of RD**—RD (0.5 mg/ml) was incubated at 20 °C with L-1-tosylamido-2-phenylethyl chloromethyl ketone-treated bovine trypsin (Sigma-Aldrich) at a ratio of 1:100 (w/w) in a buffer containing 0.1 M NaCl, 20 mM MOPS/NaOH, pH 7.0, 1 mM MgCl<sub>2</sub>, and 0.1 mM EGTA. The samples were digested in the presence and absence of 0.2 mM CaCl<sub>2</sub> for 0–30 min. At predetermined times aliquots were removed, and 1 mM phenylmethylsulfonyl fluoride was added. The fractions were immediately boiled in SDS sample buffer and separated by 15% SDS-PAGE.

## RESULTS

**Sequence Analysis of the Light Chains and Design of Mutant ELCs**—The primary structure of *Physarum* ELC and RLC is more homologous with calmodulin (40% sequence identity with vertebrate CaM) than with myosin light chains of higher eukaryotes (30–32 and 27–28% identity with metazoan ELCs and RLCs, respectively). *Physarum* LCs has the highest homology with light chains of *Dictyostelium* myosin II (65 and 53% sequence identity in the case of ELC and RLC, respectively). Based on the amino acid sequence of *Physarum* ELC, EF-hand I, III, and IV are predicted to bind Ca<sup>2+</sup> (Table I). EF-hand I and III have regular, CaM-like binding loops, whereas EF-hand IV, termed as “ancestral” EF-hand, was also considered as a potential Ca<sup>2+</sup>-binding site (17). The 12-residue loop of a canonical EF-hand provides seven coordination positions for Ca<sup>2+</sup> (27, 28). The amino acid, usually glutamic acid, at the last position (-z) plays a central role in coordinating the calcium in a bidentate manner by its side chain oxygens (29) such that its mutation abolishes the Ca<sup>2+</sup> binding of canonical EF-hands (30). To localize and characterize the Ca<sup>2+</sup>-binding site we have constructed ELCs containing point mutations in EF-hand I, -II, and -IV. Glutamic acid in the -z position of the Ca<sup>2+</sup>-binding loop of motives I and III was changed to alanine in E26A ELC and E97A ELC, respectively. We have also designed a triple mutant D15A/D17A/E26A ELC containing two additional mutations at the x and y positions to ensure complete loss of binding capacity. For studying the metal binding loop of motif IV the double mutant S124A/D126A ELC was constructed. Sequence analysis of *Physarum* RLC suggested that EF-hand I of RLC cannot be a functional divalent cation-binding site since it contains a glycine in the -z position of the binding loop.

**Expression and Purification of Recombinant Light Chains and Regulatory Domain**—The wild-type and mutant ELCs, the C- and N-terminal domains of ELC, RLC, and *Dictyostelium* ELC, were expressed in *E. coli* to investigate their Ca<sup>2+</sup>-binding properties. Recombinant *Physarum* myosin RD was produced by co-expressing ELC, RLC, and the HC fragment (residues 771–841) in *E. coli* (see “Experimental Procedures”). The RLC and ELC (mutant or wild type) co-purified with the HC fragment containing a His<sub>6</sub> affinity tag (see Fig. 6, 0 min), suggesting that the three polypeptide chains can assemble into RD in the bacterial cell and that mutations of ELC do not affect binding of the light chains to the heavy chain fragment. The average yields of RDs and LCs were 15–20 and 35–45 mg of protein/liter of culture media, respectively.

**Localization and Characterization of the Ca<sup>2+</sup>-binding Site by Direct Binding Assay**—Ca<sup>2+</sup> binding measurements are summarized in Figs. 1–3, and macroscopic dissociation constants, calculated by the Adair-Klotz equation (see “Experimental Procedures”), are summarized in Table II. The wild-type ELC and RD bind one Ca<sup>2+</sup> (mol/mol). The RD showed considerably higher Ca<sup>2+</sup> affinity than those of ELC; however, the divalent cation-binding site is not highly specific to Ca<sup>2+</sup> in either molecule (Fig. 1). Examination of recombinant *Dictyostelium* ELC by flow dialysis also indicated the presence of one divalent cation-binding site, whereas *Physarum* RLC did not show any metal binding (Fig. 2). Binding studies of the two separate lobes of *Physarum* ELC revealed that the Ca<sup>2+</sup>-binding site is located in the N-terminal domain (Fig. 2). In accordance with these results, the mutants E97A ELC and S124A/D126A ELC (EF-hand III and IV mutants, respectively) show similar calcium-binding capacity to the wild type ELC. Only partial loss of Ca<sup>2+</sup> binding was observed in the mutant E26A ELC (EF-hand I mutant), although the glutamic acid in the -z position of a canonical metal binding loop normally provides bidentate coordination for Ca<sup>2+</sup>. Introduction of two additional mutations in the first and third position of loop I (D15A/D17A/E26A ELC) completely abolished Ca<sup>2+</sup> binding to both ELC and RD, indicating that EF-hand I of ELC is the only binding site for divalent cations in *Physarum* myosin (Fig. 3). Ca<sup>2+</sup>-binding studies of myosin by equilibrium dialysis showed that *Physarum* myosin binds 2 mol of Ca<sup>2+</sup>/mol of protein non-cooperatively with a macroscopic dissociation constant of 4.4 μM in the presence of 2 mM MgCl<sub>2</sub> (Fig. 1, inset).

**Transient Kinetics of Divalent Cation Dissociation**—Because the metal-binding site in the ELC of *Physarum* myosin has moderate selectivity for Ca<sup>2+</sup> (see Fig. 1 and Table II) it could be occupied by Mg<sup>2+</sup> under physiological conditions. To assess whether bound Mg<sup>2+</sup> could be exchanged at a physiologically relevant time scale upon increase in Ca<sup>2+</sup> concentration, dissociation rates of the two ions from ELC and RD were measured by stopped flow fluorimetry. The results are summarized in Table III and Fig. 4. The divalent cation-sensitive fluorescence of IAEDANS-labeled ELC was used to determine the Ca<sup>2+</sup> and Mg<sup>2+</sup> dissociation rates of ELC. Wild-type and mutant ELCs containing a single cysteine residue (Cys-10) in the A helix of EF-hand I were stoichiometrically labeled with 1,5-IAEDANS. Ca<sup>2+</sup>- or Mg<sup>2+</sup>-saturated IAEDANS-labeled light chains were mixed with an excess of EDTA. The association of divalent cations with EDTA is fast enough ( $k_{on}$  of EDTA ≈ 4.5 × 10<sup>6</sup> M<sup>-1</sup>s<sup>-1</sup> for Ca<sup>2+</sup> (31)) that the rate-limiting steps in these experiments were the dissociation of Ca<sup>2+</sup>/Mg<sup>2+</sup> from ELC with a  $k_{off}$  value of 671.1 s<sup>-1</sup> for Ca<sup>2+</sup> and with a nearly 40-fold lower value for Mg<sup>2+</sup> ( $k_{off}$  = 18.1 s<sup>-1</sup>). Ca<sup>2+</sup> off-rate of RD was determined by mixing the Ca<sup>2+</sup>-saturated RD with excess of the calcium indicator Quin 2. The association of Ca<sup>2+</sup> with Quin 2 is a fast, diffusion controlled process with a  $k_{on}$  ≈

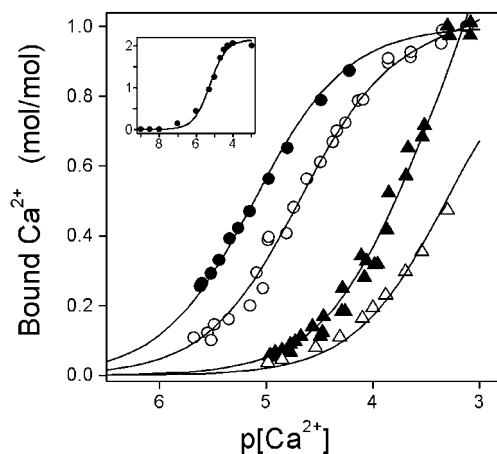


FIG. 1.  $\text{Ca}^{2+}$ -binding to *Physarum* ELC, RD and myosin.  $\text{Ca}^{2+}$  binding to ELC and RD was measured in the presence (triangles) and absence (circles) of 2 mM  $\text{MgCl}_2$  by flow dialysis with  $^{45}\text{CaCl}_2$  in 0.1 M NaCl, 20 mM MOPS/NaOH pH 7.0 at 25 °C. ● and ▲, RD; ○ and △, ELC. Inset,  $\text{Ca}^{2+}$  binding to the *Physarum* myosin was measured in the presence of 2 mM  $\text{MgCl}_2$  by equilibrium dialysis method in a buffer containing 50 mM NaCl, 20 mM MOPS/NaOH pH 7.0, 3 mM  $\text{NaN}_3$  at 22 °C. Solid lines show the best-fit curves to Adair-Klotz equation (Experimental Procedures) for each set of data.

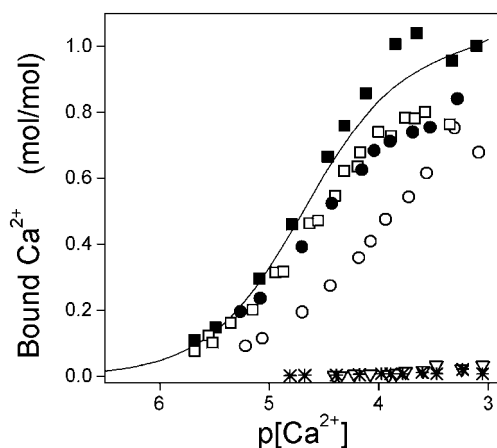


FIG. 2.  $\text{Ca}^{2+}$  binding to RLC and wild-type or mutant ELCs.  $\text{Ca}^{2+}$  binding was measured under the same conditions in the absence of  $\text{Mg}^{2+}$  as shown in Fig. 1. ■, E97A ELC (domain III mutant); □, S124A/D126A ELC (domain IV mutant); ○, N-terminal lobe of ELC; \*, C-terminal lobe of ELC; ●, *Dictyostelium* ELC; ▽, *Physarum* RLC. The solid line represents the best-fit curve to the binding data of wild-type ELC.

$10^9 \text{ M}^{-1}\text{s}^{-1}$  (32); therefore, the rate-limiting step was  $\text{Ca}^{2+}$  dissociation from the RD. The observed  $k_{\text{off}}$  value of  $2.03 \text{ s}^{-1}$  for  $\text{Ca}^{2+}$  dissociation from the RD is similar to the  $\text{Ca}^{2+}$  off-rates of a  $(\text{Ca}^{2+})_4\text{CaM}$ -target peptide complex (33).

The  $k_{\text{off}}$  value for  $\text{Mg}^{2+}$  was obtained by measuring the rate of chasing of  $\text{Mg}^{2+}$  with  $\text{Ca}^{2+}$  from the RD. The change in  $\text{Ca}^{2+}$  concentration was followed with the low affinity calcium indicator, Calcium Green 5N, suitable for fast kinetic studies ( $k_{\text{off}} = 10^{-4} \text{ s}^{-1}$  for  $\text{Ca}^{2+}$  (31)).  $\text{Mg}^{2+}$  dissociates from the  $\text{Mg}^{2+}$ -RD complex with a value of  $1.08 \text{ s}^{-1}$ , which is nearly 20-fold faster than  $k_{\text{off}}$  of  $\text{Mg}^{2+}$  from the divalent metal-binding site of RLC in skeletal muscle myosin S1 (34). Second order rate constants ( $k_{\text{on}}$ ) for  $\text{Ca}^{2+}$  and  $\text{Mg}^{2+}$  binding to ELC and RD were also calculated from the dissociation rate constants and macroscopic dissociation constants, determined by flow dialysis method (see “Experimental Procedures”).  $\text{Mg}^{2+}$  binding to both ELC and RD is 10–20-fold slower process compared with the rate of association of  $\text{Ca}^{2+}$  with ELC and RD, respectively (Table III).

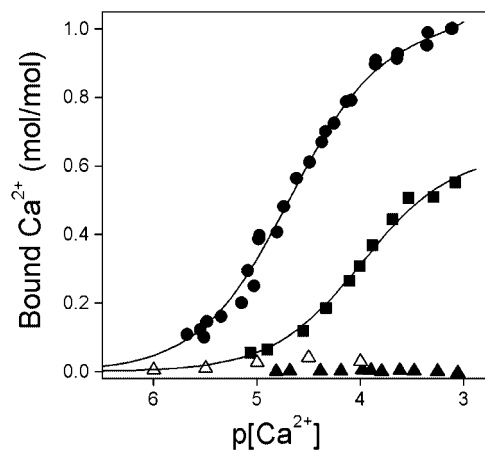


FIG. 3. Effect of mutations of metal binding loop I on the  $\text{Ca}^{2+}$ -binding properties of recombinant ELCs and RD. Flow dialysis experiments were carried out under the same conditions as shown in Fig. 1.  $\text{Ca}^{2+}$  binding of RD containing D15A/D17A/E26A was measured by equilibrium dialysis method (see “Experimental Procedures”). ●, wild-type ELC; ■, E26A ELC; ▲, D15A/D17A/E26A ELC; △, RD containing D15A/D17A/E26A ELC. Solid lines were fitted to the binding data of wild-type and E26A ELC as indicated in Fig. 1.

TABLE II  
Divalent cation binding to wild-type and mutant ELCs, RD and myosin

	Macroscopic dissociation constants		
	$K_{\text{Ca}^{2+}}$		$K_{\text{Mg}^{2+}}$
	0 mM $\text{Mg}^{2+}$	2 mM $\text{Mg}^{2+}$	
	$\mu\text{M}$		
Wild-type ELC <sup>a</sup>	20	490	88
E26A ELC <sup>a</sup>	190		
D15A/D17A/E26A ELC <sup>a</sup>	0		0
RD <sup>a</sup>	7.3	190	77
Myosin <sup>b</sup>	3.9 <sup>c</sup>	4.4	1400 <sup>c</sup>
<i>Dictyostelium</i> ELC	34		

<sup>a</sup> Measured by flow dialysis.

<sup>b</sup> Measured by equilibrium dialysis.

<sup>c</sup> Calculated using  $\text{Ca}^{2+}$ -binding data from Kohama and Kendrics-Jones (5).

TABLE III  
Kinetic parameters for dissociation and binding of divalent cations as measured by stopped flow experiments

	$k_{\text{off}}$		$k_{\text{on}}^a$	
	$\text{Ca}^{2+}$	$\text{Mg}^{2+}$	$\text{Ca}^{2+}$	$\text{Mg}^{2+}$
	$\text{s}^{-1}$		$\text{M}^{-1} \text{s}^{-1}$	
<i>Physarum</i> ELC	671.1	18.1	$3.36 \times 10^6$	$2.06 \times 10^5$
<i>Physarum</i> RD	2.03	1.08	$2.78 \times 10^5$	$1.40 \times 10^4$

<sup>a</sup> Second order rate constants for binding of divalent cations to ELC and RD were calculated by  $k_{\text{on}}/K_d$ , where dissociation constants ( $K_d$ ) were determined by flow dialysis experiments.

**Steady-state Fluorescence Studies**—To examine the conformational changes induced by divalent cation binding, steady-state fluorescence studies were performed on both ELC and RD. The microenvironment of the 1,5-IAEDANS-labeled cysteine in wild-type ELC is markedly influenced by metal binding, monitored by changes of AEDANS fluorescence (Fig. 5). The fluorescence titration curve has similar shape as the plot of direct  $\text{Ca}^{2+}$  binding. The addition of  $\text{Ca}^{2+}$  or  $\text{Mg}^{2+}$  to the labeled D15A/D17A/E26A ELC did not affect the fluorescence. EF-hand III and IV mutant ELCs (E97A ELC and S124A/D126A ELC) had a similar fluorescence profile to the wild type upon increasing the  $\text{Ca}^{2+}$  level (not shown).  $\text{Ca}^{2+}$ -induced conformational change of RD was also detected by intrinsic Trp

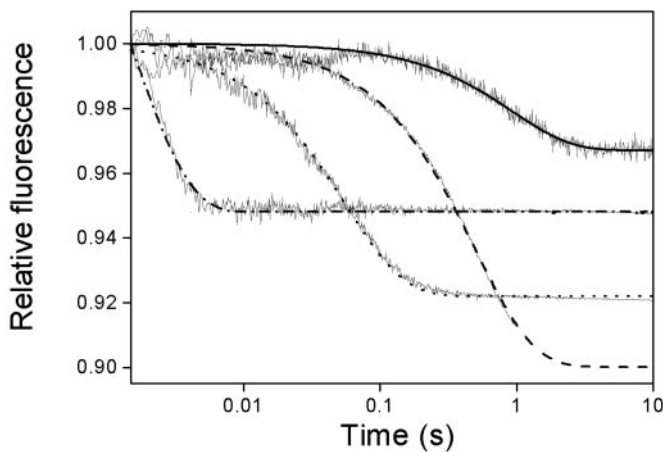


FIG. 4. Dissociation of  $\text{Ca}^{2+}$  and  $\text{Mg}^{2+}$  from *Physarum* ELC and RD monitored by stopped-flow method. Dashed and dotted line, single exponential curve fitted to the data set of EDTA induced  $\text{Ca}^{2+}$  release from IAEDANS-labeled ELC. One syringe of the stopped-flow apparatus contained  $1 \mu\text{M}$  labeled ELC and  $0.5 \text{ mM}$   $\text{CaCl}_2$ , and the other contained  $5 \text{ mM}$  EDTA. Dotted line, single exponential function fitted to the transient of EDTA induced  $\text{Mg}^{2+}$  dissociation from labeled ELC. Syringe A contained  $1 \mu\text{M}$  ELC, and  $1 \text{ mM}$   $\text{MgCl}_2$ , and syringe B contained  $5 \text{ mM}$  EDTA. Dashed line, single exponential curve fitted to data set of  $\text{Ca}^{2+}$  release from RD.  $\text{Ca}^{2+}$ -bound RD was mixed with fluorescent  $\text{Ca}^{2+}$  indicator Quin 2. Initial concentrations in syringes are  $47 \mu\text{M}$  RD and  $100 \mu\text{M}$   $\text{CaCl}_2$  (syringe A) and  $200 \mu\text{M}$  Quin 2 (syringe B). Solid line, single exponential function fitted to data set of  $\text{Mg}^{2+}$  dissociation from RD. The release of  $\text{Mg}^{2+}$  was monitored by measuring the rate of chasing of  $\text{Mg}^{2+}$  with  $\text{Ca}^{2+}$  from RD, and the change of  $\text{Ca}^{2+}$  concentration was detected with the low affinity calcium indicator Calcium Green 5N. Syringe A contained  $47 \mu\text{M}$  RD and  $1 \text{ mM}$   $\text{MgCl}_2$ , and syringe B contained  $200 \mu\text{M}$   $\text{CaCl}_2$  and  $1 \mu\text{M}$  Calcium Green 5N. The observed relative changes of fluorescence are shown on logarithmic time base. All experiments were carried out in  $50 \text{ mM}$  NaCl,  $50 \text{ mM}$  HEPES/NaOH, pH 7.6, and  $0.1 \text{ mM}$  DTT at  $22^\circ\text{C}$  with equal syringe volumes.

fluorescence measurements. The four Trp residues of *Physarum* RD are located in the heavy chain fragment; three of them are clustered at the RLC binding region, whereas the fourth Trp is in the first IQ motif, which binds ELC. The observed 5.4% change in fluorescence is likely due to the latter.  $\text{Mg}^{2+}$  binding induces a smaller fluorescence change in ELC (or RD) (Fig. 5.); however, this cation does not have an inhibitory effect on the activity of *Physarum* myosin (5).

**Limited Proteolysis**—Limited proteolysis of RD with trypsin was performed in the presence and absence of  $\text{Ca}^{2+}$  (Fig. 6). As the time course of the digestions shows, the first event was the cleavage of the HC fragment of RD, presumably just after the His<sub>6</sub> tag, where a thrombin cleavage site is found, followed by the further fragmentation of the HC. Subsequently, the cleavage of ELC and then that of RLC was observed. The cleavage of ELC, similar to the fragmentation of HC, was slower in the presence of  $\text{Ca}^{2+}$ , demonstrating the diminished accessibility of trypsin to the internal cleavage sites as a consequence of  $\text{Ca}^{2+}$  binding.

#### DISCUSSION

The oscillatory cytoplasmic streaming in *Physarum* plasmodia is thought to be powered by a conventional myosin whose activity is inhibited by an increase of  $\text{Ca}^{2+}$  concentration.  $\text{Ca}^{2+}$  could regulate the activity of plasmodial actomyosin through several mechanisms, one of which is the direct  $\text{Ca}^{2+}$  binding to myosin (5). ELC was suggested to be the  $\text{Ca}^{2+}$ -receptive subunit of *Physarum* myosin (15–17). Indeed, we confirmed these results by flow dialysis measurements of recombinant ELC and RD; both contain one  $\text{Ca}^{2+}$ -binding site. Furthermore, we localized the regulatory  $\text{Ca}^{2+}$  site in the first EF-hand of ELC. Scallop myosin, the only other known  $\text{Ca}^{2+}$ -binding conventional myosin, has the regulatory site located also in EF-hand

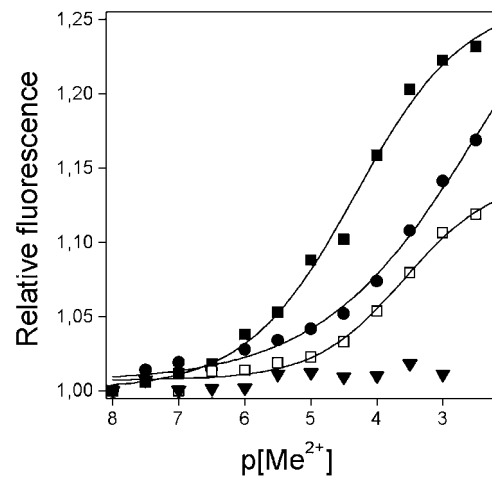


FIG. 5. Effect of  $\text{Ca}^{2+}$  and  $\text{Mg}^{2+}$  on the fluorescence of IAE-DANS-labeled ELC. Fluorescence of wild-type ELC was measured in a buffer containing  $50 \text{ mM}$  NaCl,  $20 \text{ mM}$  MOPS/NaOH, pH 7.2,  $0.1 \text{ mM}$  DTT at  $22^\circ\text{C}$  as a function of  $\text{Ca}^{2+}$  concentration (■),  $\text{Mg}^{2+}$  concentration (●), and  $\text{Ca}^{2+}$  in the presence of  $2 \text{ mM}$   $\text{MgCl}_2$  (□). ▼, fluorescence of D15A/D17A/E26A ELC as a function of  $\text{Ca}^{2+}$ .

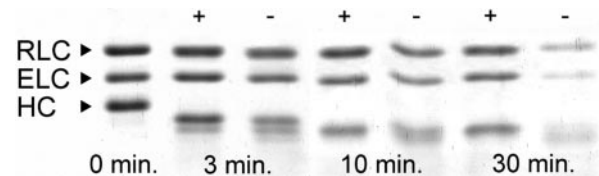


FIG. 6. Limited proteolysis of RD. Tryptic digestion of RD was digested with L-1-tosylamido-2-phenylethyl chloromethyl ketone-treated bovine trypsin at a ratio of 1:100 (w/w)  $0.1 \text{ M}$  NaCl,  $20 \text{ mM}$  MOPS/NaOH, pH 7.0,  $1 \text{ mM}$   $\text{MgCl}_2$ ,  $0.1 \text{ mM}$  EGTA in the presence (+) and absence (–) of  $0.2 \text{ mM}$   $\text{CaCl}_2$ . Samples were taken after 3, 10, 30 min of incubation with trypsin, inactivated by  $1 \text{ mM}$  phenylmethylsulfonyl fluoride, and separated by 15% SDS-PAGE.

I of ELC (35). Unlike the calmodulin-like canonical EF-hand I of *Physarum* ELC, the triggering site of scallop myosin has a unique EF-hand sequence and an unusual structure. The  $\text{Ca}^{2+}$ -binding loop is shorter (9 versus 12 residues) and has different ligand positions than in regular EF-hands (10, 11). The very fact that the  $\text{Ca}^{2+}$ -binding site is located in the same EF-hand motif raises the possibility that there could be common features in the structural basis of the two but oppositely regulated myosins. Flow dialysis experiments of RLC verified our prediction that *Physarum* RLC does not have a functional bivalent cation-binding site. This feature seems to be a characteristic of all lower eukaryotic RLCs (36). Interestingly we found that *Dictyostelium* ELC also contains a bivalent cation-binding site. However, the enzymatic activity of *Dictyostelium* myosin II is regulated by phosphorylation (37); therefore, we assume that this binding site is either not specific for  $\text{Ca}^{2+}$ , or even if it preferentially binds  $\text{Ca}^{2+}$ , the binding site has only a structural and non-regulatory role. Based on the high sequence similarity between *Physarum* and *Dictyostelium* ELC, the binding site is presumably located in EF-hand I of both ELCs.

*Physarum* ELC and RD bind  $\text{Ca}^{2+}$  with a macroscopic dissociation constant of  $20$  and  $7.3 \mu\text{M}$ , respectively (Table II).  $\text{Ca}^{2+}$  has three times higher affinity to RD than to the isolated ELC, which could be explained by stabilizing interactions of the binding EF-hand with the other two chains of the RD complex. Interestingly, the  $\text{Mg}^{2+}$  affinity of RD is approximately the same as that of the isolated ELC. In the case of scallop myosin,  $\text{Ca}^{2+}$  binds with high affinity and selectivity to the EF-hand I of ELC only in the three-chain complex of RD (38). *Physarum* myosin shows an  $\sim 50$ -fold higher  $\text{Ca}^{2+}$  affinity over RD in the



presence of 2 mM  $\text{MgCl}_2$  (the apparent dissociation constant of  $\text{Ca}^{2+}$  is 4.4  $\mu\text{M}$ ; see Table II and Fig. 1, *inset*), indicating that the divalent cation-binding site has considerably higher  $\text{Ca}^{2+}$  discrimination in the full-size myosin molecule ( $K_d$  of  $\text{Mg}^{2+}$  is greater than 1 mM in myosin). Thus, not only the interchain interactions within the RD but also the presence of interhead and/or motor domain-ELC interactions could increase the  $\text{Ca}^{2+}$  selectivity of the binding site. The  $\text{Ca}^{2+}$  affinity of *Physarum* myosin is in the same range as the average  $\text{Ca}^{2+}$  affinity to the EF-hands of CaM (39). The interplasmoidal concentration of  $\text{Ca}^{2+}$  and  $\text{Mg}^{2+}$  is in the micromolar range and  $\sim 1$  mM, as determined by injecting aequorin into plasmodia (40) and by an NMR technique (41), respectively. Therefore, it seems likely that *in vivo* the binding site of myosin is at least partially saturated by  $\text{Mg}^{2+}$ . It is worth noting that CaM does not have an absolute selectivity for  $\text{Ca}^{2+}$  either.  $\text{Mg}^{2+}$  was shown to compete with  $\text{Ca}^{2+}$  at or near physiological conditions; however,  $\text{Mg}^{2+}$  binds to the EF-hands of CaM without inducing the conformational changes responsible for its biological functions (42–44).

Regarding the physiological relevance of the competitive binding of the two divalent cations to *Physarum* myosin, it was important to investigate the exchange rate between  $\text{Ca}^{2+}$  and  $\text{Mg}^{2+}$ . As determined by transient kinetic measurements, the calcium off-rate of ELC and RD is 671.1 and 2.03  $\text{s}^{-1}$ , respectively. Similar dissociation rates were observed in the case of CaM and CaM-target peptide complexes (33). The estimated  $\text{Ca}^{2+}$  off-rate of scallop RD ( $\sim 25$   $\text{s}^{-1}$ ) is faster compared with that of *Physarum* RD (45). However, the difference is only 10-fold, and it should be taken into account that the cytoplasmic streaming driven by *Physarum* myosin is a much slower process than contraction of scallop adductor muscle. The replacement of  $\text{Mg}^{2+}$  by  $\text{Ca}^{2+}$  at the potential regulatory site of ELC on the increase of intracellular  $\text{Ca}^{2+}$  concentration is limited by the rate of  $\text{Mg}^{2+}$  dissociation, a value of 1.08  $\text{s}^{-1}$ . Apparently, this  $\text{Mg}^{2+}$ - $\text{Ca}^{2+}$  exchange rate is considerable faster than that observed at the nonspecific divalent cation-binding sites of scallop and chicken skeletal muscle RLC (0.05 and 0.057  $\text{s}^{-1}$ , respectively (34)) and also faster than the change in direction of cytoplasmic streaming (several seconds (12)); therefore, we conclude that the  $\text{Ca}^{2+}$  binding to *Physarum* ELC could act as a regulatory signal despite its limited selectivity.

The fact that direct  $\text{Ca}^{2+}$  binding to *Physarum* myosin inhibits its activity is unique among conventional myosins, but a similar type of regulation exists in many unconventional myosins where usually CaM is the light chain subunit. By increasing the  $\text{Ca}^{2+}$  concentration, CaMs may dissociate from some unconventional myosins, but others are inhibited without any loss of CaM (46–49). In case of myosin IC, the C-terminal lobe of CaM was found to be responsible for inhibition of motor activity (8). The molecular mechanism of  $\text{Ca}^{2+}$  regulation must be different in the *Physarum* conventional myosin, where the inhibitory binding site is located in the N-terminal lobe of ELC. This is the first known example where a canonical EF-hand in the N-terminal domain of a light chain or CaM is involved in the inhibitory regulation of myosin activity.

Models of apo-CaM-myosin IQ complexes show that the N-terminal domain of CaM is in a closed conformation (50, 51). Based on the above structural models and the high sequence similarity of the *Physarum* myosin LCs to CaM we assume that the N-terminal domain of *Physarum* ELC is also in a closed conformation in the absence of  $\text{Ca}^{2+}$ . Moreover, our results suggest that the site remains in the closed state upon  $\text{Ca}^{2+}$  binding since the 12th residue of the binding loop ( $-z$  position), in contrast to the standard EF-hands, does not take part in

metal coordination; a replacement of the  $-z$  position Glu to Ala did not abolish  $\text{Ca}^{2+}$  binding, *i.e.* the characteristic closed-to-open transition of canonical EF-hands probably does not occur in the N-terminal lobe of *Physarum* ELC. Structural models of scallop RD show that the N-terminal domain of ELC is also in a closed state both in the  $\text{Ca}^{2+}$ -bound and the  $\text{Ca}^{2+}$ -free form (10, 11).<sup>2</sup> Despite the opposite effect of  $\text{Ca}^{2+}$  binding on the motor activity of scallop and *Physarum* conventional myosins (activation *versus* inhibition) and the relatively low sequence similarities of the two  $\text{Ca}^{2+}$ -binding ELCs, the two myosin motors have a common structural basis for  $\text{Ca}^{2+}$  regulation; that is, a closed N-terminal lobe of ELC both in the absence and presence of  $\text{Ca}^{2+}$ . Nevertheless, the mechanism underlying  $\text{Ca}^{2+}$  regulation in the two conventional myosins is strikingly different; the scallop myosin RD acts as a *bona fide* on/off  $\text{Ca}^{2+}$  switch, whereas the  $\text{Ca}^{2+}$  binding to *Physarum* RD has only a modulatory effect (partial inhibition (5)) on the motor activity.

Steady-state fluorescence and limited proteolysis studies indicate that  $\text{Ca}^{2+}$  binding affects both the microenvironment of the binding site (as shown by fluorescence studies) and the overall structure of the RD (as shown by the decreased accessibility of tryptic sites of RD in the presence of  $\text{Ca}^{2+}$ ). The latter results could be interpreted as a decrease in the internal mobility of the RD and/or changes in the interactions between and/or within the three chains of the regulatory complex. Preliminary results using recombinant myosin fragments indicate that  $\text{Ca}^{2+}$  inhibition of *in vitro* motility is achieved only by a double-headed heavy meromyosin construct, whereas the single-headed subfragment-1 is not regulated,<sup>3</sup> suggesting that head-head and/or head-rod interactions could contribute to the inhibitory state. In case of the  $\text{Ca}^{2+}$ - and phosphorylation-activated conventional myosins (scallop and smooth muscle myosins, respectively), head-head and head-rod interactions stabilize the motor protein in the low activity off state, which is an asymmetric structure where the two heads interact and immobilize each other (52, 53).

This work provides evidence that the inhibitory  $\text{Ca}^{2+}$ -binding site of *Physarum* myosin is located in the first EF-hand of ELC. Our results indicate that  $\text{Ca}^{2+}$  and  $\text{Mg}^{2+}$  compete for the binding site. However, the exchange of divalent cations is fast enough compared with the time scale required to regulate the cytoplasmic streaming; consequently, we conclude that the inhibitory system could operate in the plasmodia of *Physarum* myosin. We have recently obtained crystals of *Physarum* myosin RD, and its high resolution structure is currently being refined.<sup>4</sup> The structure confirms the localization of the  $\text{Ca}^{2+}$ -binding site in the first EF-hand motif of ELC and also verifies the surprising finding of this work that the  $\text{Ca}^{2+}$ -saturated N-terminal lobe of ELC is in a closed conformation. Detailed analysis of the *Physarum* myosin RD structure could shed more light of this unique  $\text{Ca}^{2+}$  inhibitory mechanism, and its comparison with the scallop regulatory switch could deepen our general understanding of the  $\text{Ca}^{2+}$  regulation of conventional myosins.

*Acknowledgments*—We thank Dr. Clive Bagshaw for allowing us to use his stopped flow apparatus. We also thank Drs. A. G. Szent-Györgyi and G. Hegyi for valuable suggestions and reading the manuscript.

#### REFERENCES

1. Sellers, J. R. (2000) *Biochim. Biophys. Acta* **1496**, 3–22
2. Kawasaki, H., and Kretsinger, R. H. (1994) *Protein Profile*, Vol. 1, pp. 343–351, Academic Press Ltd., London

<sup>2</sup> C. Cohen, personal communication.

<sup>3</sup> H. Kawamichi, A. Nakamura, L. Nyitray, and K. Kohama, unpublished results.

<sup>4</sup> J. Debreczeni, L. Farkas, K. Kohama, and L. Nyitray, unpublished results.

3. Trybus (1991) *Cell Motil. Cytoskeleton* **18**, 81–85
4. Szent-Györgyi, A. G., Kalabokis, V. N., and Perreault-Micale, C. L. (1999) *Mol. Cell. Biochem.* **190**, 55–62
5. Kohama, K., and Kendrick-Jones, J. (1986) *J. Biochem. (Tokyo)* **99**, 1433–1446
6. Kohama, K., Kohno, T., Okagaki, T., and Shimmen, T. (1991) *J. Biochem. (Tokyo)* **110**, 508–513
7. Wolenski, J. S. (1995) *Trends Cell Biol.* **5**, 310–316
8. Zhu, T., Beckingham, K., and Ikebe, M. (1998) *J. Biol. Chem.* **273**, 20481–20486
9. Yokota, E., Muto, S., and Shimmen, T. (1999) *Plant Physiol.* **119**, 231–240
10. Xie, X., Harrison, D. H., Schlichting, I., Sweet, R. M., Kalabokis, V. N., Szent-Györgyi, A. G., and Cohen, C. (1994) *Nature* **368**, 306–312
11. Houdusse, A., and Cohen, C. (1996) *Structure (Lond.)* **4**, 21–32
12. Kamiya, N. (1981) *Annu. Rev. Plant Physiol.* **32**, 205–236
13. Kessler, D., Eisenlohr, L. C., Lathwell, M. J., Huang, J., Taylor, H. C., Godfrey, S. D., and Spady, M. L. (1980) *Cell Motil.* **1**, 63–71
14. Kohama, K., Uyeda, T. O. P., Takano-Ohmuro, H., Tanaka, T., Yamaguchi, T., Maruyama, K., and Kohama, T. (1985) *Proc. Jpn. Acad.* **61**, 501–505
15. Kohama, K., Okagaki, T., Takano-Ohmuro, H., and Ishikawa, R. (1991) *J. Biochem. (Tokyo)* **110**, 566–570
16. Ishikawa, R., Okagaki, T., Higashi-Fujime, S., and Kohama, K. (1991) *J. Biol. Chem.* **266**, 21784–21790
17. Ishikawa, R., Okagaki, T., and Kohama, K. (1992) *J. Muscle Res. Cell Motil.* **13**, 321–328
18. Chomczynski, P., and Sacchi, N. (1987) *Anal. Biochem.* **162**, 156–159
19. Nakamura, A., Okagaki, T., Takagi, T., Nakashima, K., Yazawa, M., and Kohama, K. (2000) *Biochemistry* **39**, 3827–3834
20. Camp, W. G. (1936) *Bull. Torrey Bolt. Club* **63**, 205–210
21. Hatano, S., and Oosawa, F. (1966) *Biochim. Biophys. Acta* **127**, 488–498
22. Nakashima, K., Maekawa, H., and Yazawa, M. (1996) *Biochemistry* **35**, 5602–5610
23. Nakashima, K., Ishida, H., Ohki, S. Y., Hikichi, K., and Yazawa, M. (1999) *Biochemistry* **38**, 98–104
24. Chantler, P. D., Sellers, J. R., and Szent-Györgyi, A. G. (1981) *Biochemistry* **20**, 210–216
25. Edsall, J. T., and Wyman, J. (1958) *Biophysical Chemistry*, Vol. 1, pp. 591–662, Academic Press, Inc., New York
26. Kovacs, M., Malnasi-Csizmadia, A., Wooley, R. J., and Bagshaw, C. R. (2002) *J. Biol. Chem.* **277**, 28459–28467
27. Babu, Y. S., Sack, J. S., Greenhough, T. J., Bugg, C. E., Means, A. R., and Cook, W. J. (1985) *Nature* **315**, 37–40
28. Babu, Y. S., Bugg, C. E., and Cook, W. J. (1988) *J. Mol. Biol.* **204**, 191–204
29. Strynadka, N. C., and James, M. N. (1989) *Annu. Rev. Biochem.* **58**, 951–998
30. Beckingham, K. (1991) *J. Biol. Chem.* **266**, 6027–6030
31. Naraghi, M. (1997) *Cell Calcium* **22**, 255–268
32. Quast, U., Labhardt, A. M., and Doyle, V. M. (1984) *Biochem. Biophys. Res. Commun.* **123**, 604–611
33. Brown, S. E., Martin, S. R., and Bayley, P. M. (1997) *J. Biol. Chem.* **272**, 3389–3397
34. Bennett, A. J., and Bagshaw, C. R. (1986) *Biochem. J.* **223**, 173–177
35. Fromherz, S., and Szent-Györgyi, A. G. (1995) *Proc. Natl. Acad. Sci. U. S. A.* **92**, 7652–7656
36. Collins, J. H. (1991) *J. Muscle Res. Cell Motil.* **12**, 3–25
37. Tan, J. L., Ravid, S., and Spudich, J. A. (1992) *Annu. Rev. Biochem.* **61**, 721–759
38. Kwon, H., Goodwin, E. B., Nyitray, L., Berliner, E., O'Neill-Hennessey, E., Melandri, F. D., and Szent-Györgyi, A. G. (1990) *Proc. Natl. Acad. Sci. U. S. A.* **87**, 4771–4775
39. Chin, D., and Means, A. R. (2000) *Trends Cell Biol.* **10**, 322–328
40. Ridgway, E. B., and Durham, A. C. (1976) *J. Cell Biol.* **69**, 223–226
41. Kohama, K. (1987) *Adv. Biophys.* **23**, 149–182
42. Martin, S. R., and Bayley, P. M. (2002) *Protein Sci.* **11**, 2909–2923
43. Malmendal, A., Linse, S., Evenas, J., Forsen, S., and Drakenberg, T. (1999) *Biochemistry* **38**, 11844–11850
44. Malmendal, A., Evenas, J., Thulin, E., Gippert, G. P., Drakenberg, T., and Forsen, S. (1998) *J. Biol. Chem.* **273**, 28994–29001
45. Jackson, A. P., and Bagshaw, C. R. (1988) *Biochem. J.* **251**, 515–526
46. Trybus, K. M., Kremontsova, E., and Freyzon, Y. (1999) *J. Biol. Chem.* **275**, 27448–27456
47. Yoshimura, M., Homma, K., Saito, J., Inoue, A., Ikebe, R., and Ikebe, M. (2001) *J. Biol. Chem.* **276**, 39600–39607
48. Homma, K., Saito, J., Ikebe, R., and Ikebe, M. (2001) *J. Biol. Chem.* **276**, 34348–34354
49. Collins, K., Sellers, J. R., and Matsudaira, P. (1990) *J. Cell Biol.* **110**, 1137–1147
50. Houdusse, A., Silver, M., and Cohen, C. (1996) *Structure (Lond.)* **4**, 1475–1490
51. Houdusse, A., Trybus, K., and Cohen, C. (2000) *Biophys. J.* **78**, 158a (abstr.)
52. Stafford, W. F., Jacobsen, M. P., Woodhead, J., Craig, R., O'Neill-Hennessey, E., and Szent-Györgyi, A. G. (2001) *J. Mol. Biol.* **307**, 137–147
53. Wendt, T., Taylor, D., Trybus, K. M., and Taylor, K. (2001) *Proc. Natl. Acad. Sci. U. S. A.* **98**, 4361–4366